

Article

Cosmeceutical Effects of *Ishige okamurae* Celluclast Extract

Fengqi Yang ^{1,2} , Jimin Hyun ¹, D. P. Nagahawatta ¹, Young Min Kim ³, Moon-Soo Heo ^{1,*} and You-Jin Jeon ^{1,*} ¹ Department of Marine Life Sciences, Jeju National University, Jeju 63243, Republic of Korea² Marine Science Institute, Jeju National University, Jeju 63333, Republic of Korea³ Aqua Green Technology Co., Ltd., Smart Bldg., Jeju Science Park, Cheomdan-ro, Jeju 63309, Republic of Korea

* Correspondence: msheo@jejunu.ac.kr (M.-S.H.); youjin@jejunu.ac.kr (Y.-J.J.); Tel.: +82-64-754-3475 (Y.-J.J.)

Abstract: Sulfated polysaccharides extracted from brown algae are unique algal polysaccharides and potential ingredients in the cosmeceutical, functional food, and pharmaceutical industries. Therefore, the present study evaluated the cosmeceutical effects, including antioxidant, anti-wrinkle, anti-inflammation, and photoprotective activities, of *Ishige okamurae* Celluclast extract (IOC). The IOC was abundant in sulfated polysaccharides (48.47%), polysaccharides (44.33%), and fucose (43.50%). Moreover, the IOC effectively scavenged free radicals, and its anti-inflammatory properties were confirmed in lipopolysaccharide-induced RAW 264.7 macrophages; therefore, the IOC may produce auxiliary effects by inhibiting reactive oxygen species (ROS). In vitro (Vero cells) and in vivo (zebrafish) studies further confirmed that the IOC produced a protective effect against hydrogen-peroxide-induced oxidative stress in a dose-dependent manner. In addition, the IOC suppressed intracellular ROS and apoptosis and enhanced HO-1 and SOD-1 expression through transcriptional activation of Nrf2 and downregulation of Keap1 in HaCaT cells. Furthermore, the IOC exhibited a potent protective effect against ultraviolet-B-induced skin damage and photoaging. In conclusion, the IOC possesses antioxidant, anti-inflammatory, and photoprotective activities, and can, therefore, be utilized in the cosmeceutical and functional food industries.



Citation: Yang, F.; Hyun, J.; Nagahawatta, D.P.; Kim, Y.M.; Heo, M.-S.; Jeon, Y.-J. Cosmeceutical Effects of *Ishige okamurae* Celluclast Extract. *Antioxidants* **2022**, *11*, 2442. <https://doi.org/10.3390/antiox11122442>

Academic Editors: Irene Dini and Sonia Laneri

Received: 16 November 2022

Accepted: 8 December 2022

Published: 10 December 2022

Publisher's Note: MDPI stays neutral with regard to jurisdictional claims in published maps and institutional affiliations.



Copyright: © 2022 by the authors. Licensee MDPI, Basel, Switzerland. This article is an open access article distributed under the terms and conditions of the Creative Commons Attribution (CC BY) license (<https://creativecommons.org/licenses/by/4.0/>).

Keywords: *Ishige okamurae*; Celluclast; sulfated polysaccharides; cosmeceutical effect; antioxidant activity; anti-inflammatory activity; photoprotective effect

1. Introduction

Reactive oxygen species (ROS), which are present in various forms, are physiological metabolites generated through oxygen metabolism under normal physiological conditions. Various factors, including ultraviolet-B (UVB) radiation, heavy metal ions, drugs, pollutants, and fine dust particles, promote ROS production [1–3]. However, ROS overproduction can interfere with the mitochondrial membrane potential and disrupt the cellular redox balance, resulting in the induction of oxidative stress and development of numerous diseases, including neurological disorders, cardiovascular disease, digestive diseases, and certain cancers [4,5]. As the skin is inevitably exposed to UVB rays in daily life, this can lead to oxidative damage of the skin tissues and cells. Excessive ROS accumulation leads to photoaging and inflammation of the human skin, eventually resulting in dermal malignancies [6,7]. Moreover, some cosmetics containing specific chemicals, such as heavy metals, steroids, hydroquinones, and nitrosamines, albeit effective in the short-term, can harm human health in the long-term [8]. Therefore, eco-friendly cosmetics containing natural ingredients must be developed. In recent years, cosmetic products with non-toxic and highly bioactive natural ingredients have attracted increasing research attention.

In this context, seaweeds have found wide pharmaceutical and industrial applications as natural sources of compounds because of their non-toxicity, easy cultivation, low cost, and presence of an array of active compounds, such as polysaccharides, proteins, minerals, vitamins, and pigments; therefore, seaweeds are the best candidates to replace synthetic compounds [9–11]. The majority of the algal species contain polysaccharides,

polyphenols, and peptides, and most of these compounds exhibit biological functions, such as antioxidant, antimicrobial, antitumoral, anti-inflammatory, and UVB protective effects [12,13].

Ishige okamurae is one of the most common edible brown algae. It is widely distributed in the coastal areas of East Asia and contains abundant polyphenols, fucoxanthin, diphloretrohydroxycarmalol, and ishigoside bioactive compounds [7,14,15]. Many activities of *I. okamurae* have been investigated. For instance, the ethanolic extract of *I. okamurae* was effective against particulate matter-induced skin damage and produced antibacterial effects. In addition, the protective effects of the methanolic extract of *I. okamurae* against inflammatory myopathy as well as its anti-obesity, antioxidant, and anticancer activities have been reported [11,15–17]. Although there are many studies on *I. okamurae*, there is little information available on the cosmeceutical effects of *I. okamurae*, especially the Celluclast extract. A variety of extraction technologies are widely used, such as enzyme-assisted extraction, ultra-high-pressure extraction, microwave-assisted extraction technology, and supercritical fluid extraction. Compared with organic and water extraction, enzymatic extraction has a high catalytic efficiency and is more conducive to destroying the cell walls, which can not only improve the extraction yield but also show better biological activity, which is suitable for algae extraction [18,19]. In addition, enzyme-assisted extraction technology has mild reaction conditions and is safe. Compared with microwave and ultra-high-pressure extraction technologies, it has low equipment requirements, simple operation, is solvent-free, and has a moderate cost, so it is more suitable for food and cosmetic industrial production.

To this end, in the present study, Celluclast, a food-grade carbohydrase, was used to hydrolyze *I. okamurae*, and cosmeceutical effects of the *I. okamurae* Celluclast extract (IOC) were evaluated. Specifically, combining chemical technology, zebrafish, and cellular-level research, the antioxidant, anti-inflammatory, anti-wrinkle, and photoprotective activities of the IOC were evaluated to expand the applications of this brown alga in the cosmetic industry.

2. Materials and Methods

2.1. Materials

The collagenase from clostridium histolyticum, elastase from porcine pancreas, hyaluronidase, 2',7'-dichlorodihydrofluorescein diacetate (DCFH-DA), acridine orange, 3-(4,5-dimethyl-2yl)-2,5-diphenyltetrasolium bromide (MTT), dimethyl sulfoxide (DMSO), phosphate-buffered saline (PBS), standard gallic acid, 2,2'-azino-bis(3-ethylbenzothiazoline-6-sulphonic acid) (ABTS), H₂O₂, and the Human matrix metalloproteinases (MMP)-1, 2, 9 Enzyme-Linked Immunosorbent Assay (ELISA) kit were purchased from Sigma Co. (St. Louis, MO, USA). Penicillium/streptomycin (P/S), Dulbecco's modified Eagle's medium (DMEM), Roswell Park Memorial Institute-1640 (RPMI-1640) medium, trypsin-EDTA, and fetal bovine serum (FBS) were purchased from Gibco BRL (Life Technologies, Burlington, ON, Canada). The PGE2 kit used in the experiments was purchased from R&D Systems (Minneapolis, MN, USA). Anti-heme oxygenase 1 (HO-1), anti-superoxide dismutase 1 (SOD1), and anti-nuclear factor-erythroid 2-related factor-2 (Nrf2) antibodies were purchased from Cell Signaling Technology (Beverly, MA, USA). Kelch-like ECH-associated protein 1 (keap1) and β -actin antibody were purchased from Santa Cruz Biotechnology (Santa Cruz, CA, USA). All other chemicals used in this study were of analytical grade.

2.2. Sample Extraction

I. okamurae was harvested in April 2020 from Seongsan, Jeju Island, Republic of Korea. Following immersion in water for 24 h, the algae were washed three times with tap water to remove salt, sand, and debris. The algae were then freeze-dried and crushed. Lyophilized *I. okamurae* powder (100 g) was mixed with distilled water (1 L) at pH 4.5. Next, the mixture was extracted using Celluclast (1 g) in a continuous shaking incubator for 6 h at 50 °C. Subsequently, the enzyme was inactivated (100 °C) for 15 min. The pH of the extract

was adjusted to 7.0, and the supernatant was separated using centrifugation ($12,000\times g$, 15 min, 4 °C). The supernatant was then concentrated by evaporation and stored in a -80 °C deep freezer before freeze-drying. IOC powder was obtained by freeze-drying the mentioned supernatant.

2.3. Chemical Composition Analysis

Protein content was quantified using a commercial BCA protein assay kit (Thermo Scientific, Rockford, IL, USA). Sulfate content was analyzed using the BaCl_2 gelatin method. The samples were hydrolyzed using 4 M trifluoroacetic acid for 5 h at 100 °C [20]. Gallic acid and glucose were used as the standards to evaluate the total phenolic and polysaccharide content, respectively [21,22]. The monosaccharide content of samples was determined using the Bio-LC (HPAEC-PAD system; Dionex, Sunnyvale, CA, USA) with the CarboPacTM PA1 column following pretreatment with 2 M trifluoroacetic acid. The samples were detected with the ED50 Dionex electrochemical detector using a standard containing fucose, arabinose, galactose, rhamnose, glucose, xylose, and fructose.

2.4. Radical Scavenging Assay

The radical scavenging activity was investigated using a previously published method [23]. In brief, ABTS (7 mM) and potassium persulfate (2.45 mM) were reacted in the dark for 12 h at 25 °C to generate the radicals. The ABTS and sample solutions were mixed and provided 10 min of incubation in the dark. The radical scavenging activity of the samples was evaluated at 734 nm.

2.5. Measurement of Enzyme Inhibitory Effects of IOC

2.5.1. Collagenase Inhibitory Effect Assay

The collagenase inhibitory activity was estimated using 1 mg of Azocoll with 800 μL of 0.1 M Tris-HCl buffer (pH 7.0). An amount of 100 μL of 200 units· mL^{-1} of collagenase and 100 μL of the sample were added with 1 h incubation at 43 °C. Following incubation, the mixture was centrifuged (3000 rpm, 10 min) and the supernatant was measured at 540 nm [24].

2.5.2. Elastase Inhibitory Effect Assay

The elastase inhibitory activity was estimated according to the previous method [25]. In brief, elastase was treated with a mixture of the sample and 1.015 mM N-succinyl-alanyl-alanyl-alanyl-p-nitroanilide, and 10 min of incubation was provided at 25 °C. The microplate reader (BioTek Synergy HT, BioTek Instrument, Winooski, UT, USA) was utilized to measure the absorbance at 410 nm.

2.5.3. Hyaluronidase (HAase) Inhibitory Assay

The HAase inhibitory activity was estimated following the previous method with slight modifications [26]. Briefly, the sample was mixed with HAase (10 $\text{mg}\cdot\text{mL}^{-1}$) dissolved in acetate buffer (pH 3.5) at a 1:1 ratio and provided 20 min of incubation at 37 °C. A further 20 min of incubation was provided with CaCl_2 (12.5 mM). Then, hyaluronate was treated as a substrate and provided another 40 min of incubation. Finally, the mixture solution was incubated at 100 °C for 3 min after treating NaOH (0.4 N) and potassium tetraborate (0.4 M), and 180 μL of p-dimethylaminobenzaldehyde was added at 25 °C. The microplate reader (BioTek Synergy HT) was utilized to measure the absorbance at 540 nm.

2.6. Cell Viability Analysis

RAW 264.7, Monkey kidney fibroblasts (Vero), and human keratinocyte (HaCaT) cell lines were purchased from the Korean Cell Line Bank (KCLB, Seoul, Republic of Korea). Vero cells were maintained in RPMI-1640, and RAW 264.7 and HaCaT cells were cultured in DMEM under a controlled environment (37 °C, 5% CO_2). All media contained 1% antibiotics and 10% fetal bovine serum. All cells were seeded at the density of 1×10^5 cells· mL^{-1}

in 96-well plates and cultured for 24 h. The cells were treated with varying concentrations of IOC (3.125, 6.25, 12.5, 25, 50, 100, and 200 $\mu\text{g}\cdot\text{mL}^{-1}$) and cell viability was evaluated using the MTT assay.

2.7. Effect of the IOC on H_2O_2 -Induced Intracellular ROS Production and Cell Viability

After 24 h of Vero cells seeding, different concentrations of the IOC (3.125–200 $\mu\text{g}\cdot\text{mL}^{-1}$) were treated, incubated for 24 h, and then co-treated with hydrogen peroxide (600 μM). The cytoprotective effect of the IOC against H_2O_2 -induced cell damage was assessed using cell viability. Cells were incubated with H_2O_2 for 1 h, and then 10 μL of DCFH-DA (25 $\mu\text{g}\cdot\text{mL}^{-1}$) was added and incubated for another 10 min. Excitation at 485 nm and emission at 530 nm were measured using a microplate reader (BioTek Synergy HT) [27].

2.8. Effect of the IOC NO and PGE2 Generation on Lipopolysaccharide (LPS)-Induced RAW 264.7 Macrophages

To evaluate the anti-inflammatory effect of the IOC, RAW 264.7 cells were treated with IOC for 1 h, following co-treatment with 1 $\mu\text{g}\cdot\text{mL}^{-1}$ of LPS for 23 h. Cell viability was assessed using the MTT assay. The supernatant was collected. NO and PGE2 production were analyzed using the Griess reagent and commercial ELISA kit, respectively [25].

2.9. Cytoprotective Activity of the IOC on UVB-Induced HaCaT Cells

A UVB meter containing a fluorescent bulb (wavelength 315–280 nm, peak 313 nm) was used to irradiate (30 $\text{mJ}\cdot\text{cm}^{-2}$) HaCaT cells to induce photodamage. Serum-free DMEM medium was used for the incubation of cells until analysis. The effect of the IOC (3.125–200 $\mu\text{g}\cdot\text{mL}^{-1}$) on UVB-induced photodamage was determined based on the measurement of intracellular ROS levels, apoptotic body formation, and UVB-irradiated HaCaT cell viability using the DCFH-DA assay, Hoechst 33342 staining, and MTT assay, respectively [24,28,29].

2.10. Western Blotting

The effects of the IOC on the expression of SOD-1, Nrf2, Keap1, and HO-1 were assessed using Western blotting. IOC-treated and UVB-irradiated HaCaT cells were harvested and lysed. The BCA protein assay was used to quantify protein content in the lysate and it was subjected to 7.5% sodium dodecyl sulfate (SDS)–polyacrylamide gel electrophoresis (PAGE). The proteins were transferred onto nitrocellulose membranes blocked with 5% skim milk at 27 °C. Overnight incubation of membranes with primary antibodies at 4 °C was performed following incubation with secondary antibodies (Santa Cruz Biotechnology, Paso Robles, CA, USA) for 2 h at room temperature. Bands were detected using an ECL Western blotting detection kit and photographed using the FUSION SOLO Vilber Lourmat system (Paris, France).

2.11. Determination of Metalloproteinase (MMPs) Expression Levels Using ELISA

HaCaT cells were incubated with the IOC (50, 100, and 200 $\mu\text{g}\cdot\text{mL}^{-1}$) for 2 h and washed with PBS before UVB irradiation (30 $\text{mJ}\cdot\text{cm}^{-2}$). Following UVB irradiation, the cells were incubated with serum-free DMEM for 24 h. Culture media were collected, and MMP expression levels were quantified using a commercial ELISA kit according to the manufacturer's instructions.

2.12. Origin and Maintenance of Zebrafish

Adult zebrafish were purchased from the commercial market (Jeju Aquarium, Republic of Korea). The zebrafish were separately maintained in 3 L tanks under a 14 h light/10 h dark cycle at 28.5 °C and fed twice daily (Tetra GmgH D-49304, Melle, Germany). In the morning, embryos were obtained from natural spawning through the breeding of two males and one female.

2.13. Measurement of Heart Beating Rate, Survival Rate, ROS Generation, and Cell Death in Zebrafish Embryos

The protective effect of IOC against H₂O₂ was investigated using approximately 7–9 h post-fertilization (hpf) embryos by treating IOC (50, 100, and 200 µg·mL⁻¹); controls were untreated. Following treatment for 1 h, the embryos were stimulated with H₂O₂ (5 mM), and the plate was incubated for 3 dpf. The survival rate and heart beating rate were counted according to the previously optimized method [30]. Acridine orange and DCFH-DA were utilized to evaluate the cell death and intracellular ROS generation, respectively [31]. Zebrafish larvae were photographed using a fluorescence microscope (CoolSNAP-Pro Color Digital Camera; Olympus, Japan) and the fluorescence intensity was quantified using ImageJ software (version 1.50i, NIH, USA).

2.14. Statistical Analysis

The data were analyzed using one-way ANOVA and Dunnett's multiple comparisons test by GraphPad Prism 8 (GraphPad Software, Inc., San Diego, CA, USA). All the experiments were repeated in triplicate. All data are expressed as the mean values with the standard error of the mean (SEM). $p < 0.05$ was considered significantly different.

3. Results

3.1. Chemical Composition of IOC

Chemical composition was investigated after *I. okamurae* was hydrolyzed using Cellulast. As shown in Table 1, the IOC contained 5.32 ± 0.43% protein, 3.82 ± 0.31% phenolics, 4.14 ± 0.12% sulfates, and 44.33 ± 0.65% polysaccharides. Overall, the IOC contained 48.47% sulfated polysaccharides. Furthermore, the monosaccharide content of the IOC was determined. The IOC contained 43.50% fucose, 36.39% glucose, 7.96% galactose, 11.74% xylose, 0.17% rhamnose, and 0.25% arabinose.

Table 1. Chemical composition of IOC obtained from *I. okamurae*.

Sample	IOC	
Protein content%	5.32 ± 0.43	
Phenolic content%	3.82 ± 0.31	
Sulfate content%	4.14 ± 0.12	
Polysaccharide content%	44.33 ± 0.65	
Sulfated polysaccharide%	48.47	
Monosaccharide %	Fucose	43.50
	Glucose	36.39
	Galactose	7.96
	Xylose	11.74
	Rhamnose	0.17
	Arabinose	0.25

3.2. Enzyme Inhibitory Effects of the IOC

The inhibitory effects of the IOC on commercial collagenase, elastase, and HAase were examined, and the results are presented in Figure 1. The IOC significantly and dose-dependently increased collagenase and HAase inhibitory rates. The elastase inhibition rate did not differ among the concentration groups but was significantly increased relative to that in the control sample. At the IOC concentrations of 25, 50, and 100 µg·mL⁻¹, the inhibitory rates were 18.01%, 34.11%, and 55.62% against collagenase; 18.85%, 23.20%, and 23.43% against elastase; 1.83%, 13.56%, and 40.23% against HAase, respectively. Therefore, the IOC may produce anti-wrinkle effects through the inhibition of collagenase, elastase, and HAase.

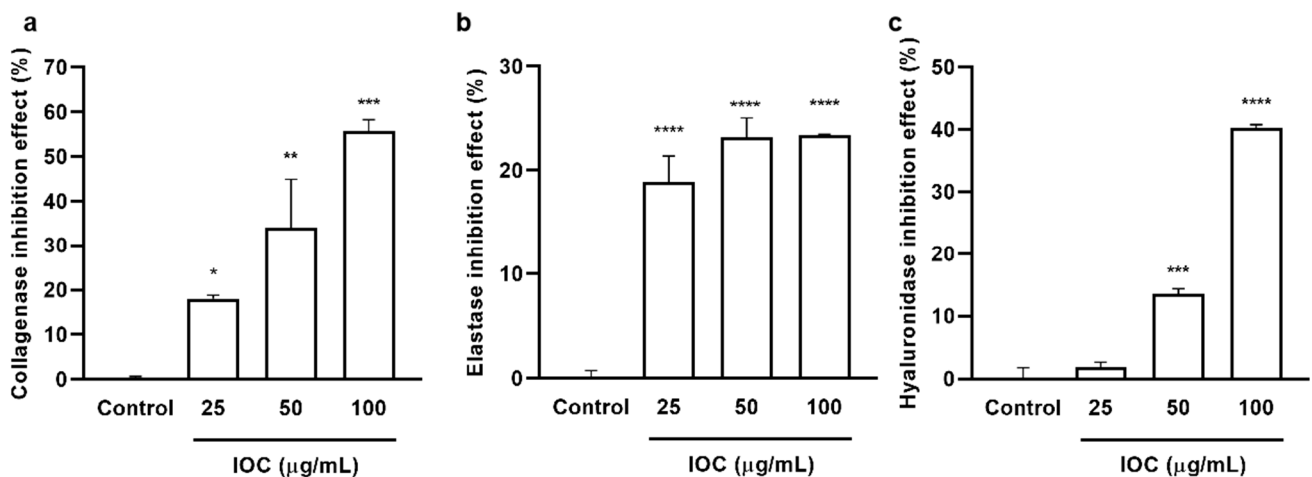


Figure 1. IOC inhibits commercial collagenase, elastase, and hyaluronidase: (a) collagenase inhibitory activity of IOC; (b) elastase inhibitory activity of IOC; (c) hyaluronidase inhibitory activity of IOC. All experiments were triplicated, and data are expressed as the mean \pm SEM. * $p < 0.05$, ** $p < 0.01$, *** $p < 0.001$, and **** $p < 0.0001$ as compared to control group.

3.3. Antioxidant Effect of the IOC

3.3.1. Free Radical Scavenging Activities of IOC

The free radical scavenging activity of the IOC was assessed using the ABTS assay. The activity of the IOC against ABTS radical cations was measured using concentrations ranging between 25 and 100 $\mu\text{g}\cdot\text{mL}^{-1}$. The percent radical scavenging activity at different concentrations of the extract is shown in Figure 2a. Significant scavenging activity was noted at 50 and 100 $\mu\text{g}\cdot\text{mL}^{-1}$ concentrations compared with the control value. In particular, the ABTS radical scavenging activity exceeded 96% at the concentration of 100 $\mu\text{g}\cdot\text{mL}^{-1}$.

3.3.2. Effect of IOC on H_2O_2 -Induced Intracellular ROS Generation and Cytotoxicity in Vero Cells

Chemical methods revealed that the IOC possesses antioxidant and anti-wrinkle activities. To further detect IOC activities, in vitro experiments were performed, and the sample concentration range was expanded. Specifically, seven concentrations (3.125–200 $\mu\text{g}\cdot\text{mL}^{-1}$) were tested to determine cytotoxicity. Cell viability did not differ significantly among the different concentrations. Hence, these concentrations (3.125–200 $\mu\text{g}\cdot\text{mL}^{-1}$) were used in further experiments. The intracellular ROS levels and viability of Vero cells following H_2O_2 stimulation are shown in Figure 2. There were no significant differences in intracellular ROS levels and cell viability between the 3.125 and 6.25 $\mu\text{g}\cdot\text{mL}^{-1}$ concentration groups; however, 12.5 to 200 $\mu\text{g}\cdot\text{mL}^{-1}$ concentration groups significantly differed from the control group and the significance of differences was dose-dependent. ROS generation tended to decrease (Figure 2b), whereas cell viability tended to increase in 12.5–200 $\mu\text{g}\cdot\text{mL}^{-1}$ concentration groups compared with values in the control group (Figure 2c).

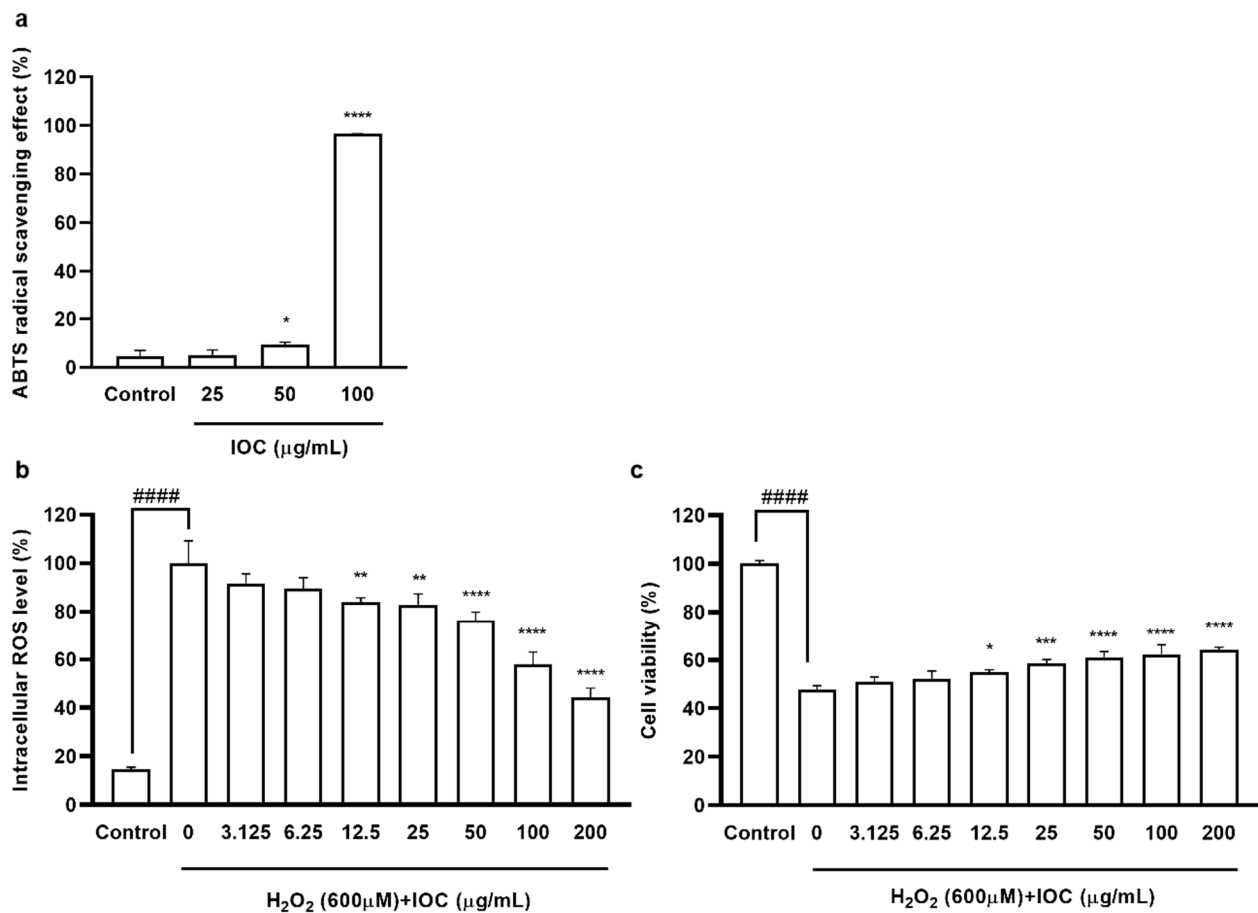


Figure 2. (a) ABTS free radical scavenging activity of IOC; (b) the intracellular ROS scavenging effect of IOC during H₂O₂ stimulated oxidative stress in Vero cells; (c) the protective effect of IOC against H₂O₂ stimulated cell death in Vero cells. All experiments were triplicated, and data are expressed as the mean ± SEM. In ABTS radical scavenging activity results: * $p < 0.05$ and **** $p < 0.0001$ as compared to control group. In intracellular ROS level and cell viability results: * $p < 0.05$, ** $p < 0.01$, *** $p < 0.001$, and **** $p < 0.0001$ as compared to the H₂O₂-treated group, and ##### $p < 0.0001$ as compared to the control group.

3.4. Effect of the IOC on NO and PGE2 Production in LPS-Induced RAW 264.7 Cells

To evaluate the anti-inflammatory effects of the IOC, we assessed the suppression of NO and PGE2 production in LPS-induced RAW 264.7 macrophages. We selected the concentration of 3.125–200 μg·mL⁻¹ based on its non-cytotoxicity to macrophages (data not shown). As shown in Figure 3, when cells were exposed to LPS, NO and PGE2 production was significantly increased but cell viability was reduced compared with the control values. NO secretion was downregulated following IOC pretreatment in a dose-dependent manner, and cell viability increased significantly following treatment with 50, 100, and 200 μg·mL⁻¹ of the IOC. In addition, the IOC (25, 50, 100, and 200 μg·mL⁻¹) inhibited LPS-induced PGE2 production in RAW 264.7 cells.

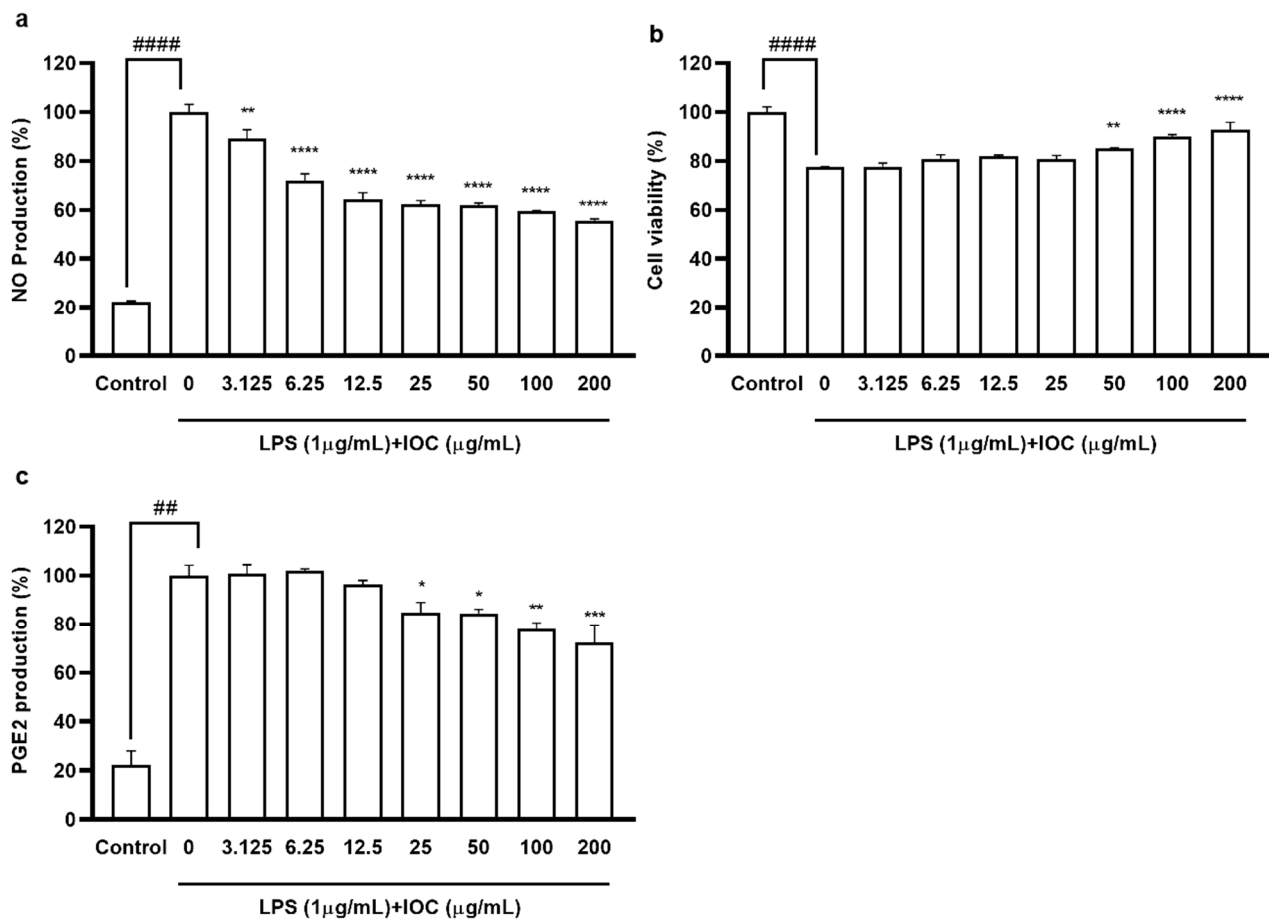


Figure 3. Effect of IOC on LPS-induced NO and PGE2 release by RAW 264.7 cells. (a) NO production inhibitory effect of IOC; (b) cytoprotective; (c) the level of PGE2. All experiments were triplicated, and data are expressed as the mean \pm SEM. * $p < 0.05$, ** $p < 0.01$, *** $p < 0.001$, and **** $p < 0.0001$ as compared to the LPS-treated group; ## $p < 0.01$ and #### $p < 0.0001$ as compared to the control group.

3.5. Effects of the IOC on Intracellular ROS Levels and Cell Viability in UVB-Induced HaCaT Cells

According to the cytotoxicity results, there were no significant differences in cell viability among 3.125 to 200 $\mu\text{g}\cdot\text{mL}^{-1}$ concentration groups, confirming that the IOC was non-toxic to HaCaT cells in this range (data not shown); thus, concentration ranges were selected for subsequent experiments. As shown in Figure 4a, UVB exposure increased intracellular ROS levels. However, treatment with the IOC reversed this effect in a dose-dependent manner. The cell viability of UVB-induced HaCaT cells was drastically reduced. However, this effect was restored following treatment with 100 and 200 $\mu\text{g}\cdot\text{mL}^{-1}$ of the IOC (Figure 4b).

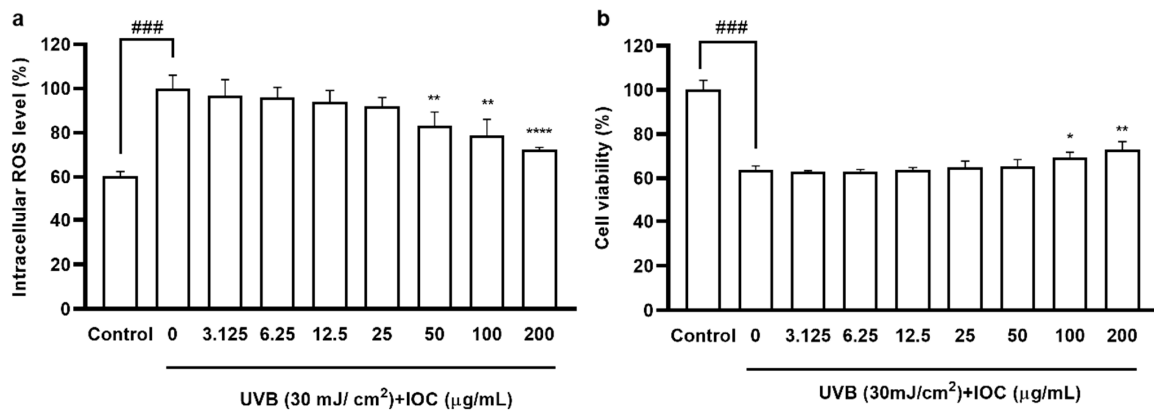


Figure 4. IOC inhibits intracellular ROS levels in UVB-irradiated HaCaT cells. (a) Intracellular ROS scavenging effect of IOC in UVB-induced HaCaT cells; (b) protective effects of IOC against UVB-irradiated HaCaT cells damage. All experiments were triplicated, and data are expressed as the mean \pm SEM. * $p < 0.05$, ** $p < 0.01$, and **** $p < 0.0001$ as compared to the UVB-irradiated group, and ### $p < 0.001$ as compared to the control group.

3.6. Effect of the IOC against UVB-Induced Apoptosis

Based on the above experimental results, higher concentrations of the IOC were found to present stronger activity, especially the concentrations from 50 to 200 $\mu\text{g}\cdot\text{mL}^{-1}$, which were significantly different from the other groups. Therefore, a concentration range of 50–200 $\mu\text{g}\cdot\text{mL}^{-1}$ was selected for subsequent experiments to verify the activity of the IOC. Figure 5 shows the protective effects of the IOC against UVB-induced apoptosis. Cells in the control group, which were untreated and not exposed to UVB, contained intact nuclei, whereas cells in the negative control group, which were untreated but exposed to UVB, showed significantly fragmented nuclei. However, nuclear fragmentation was reduced in the IOC treatment groups, especially in the 100 $\mu\text{g}\cdot\text{mL}^{-1}$ and 200 $\mu\text{g}\cdot\text{mL}^{-1}$ treatment groups. Therefore, the IOC suppresses apoptosis following UVB irradiation, protecting the HaCaT cells from UVB-induced photodamage.

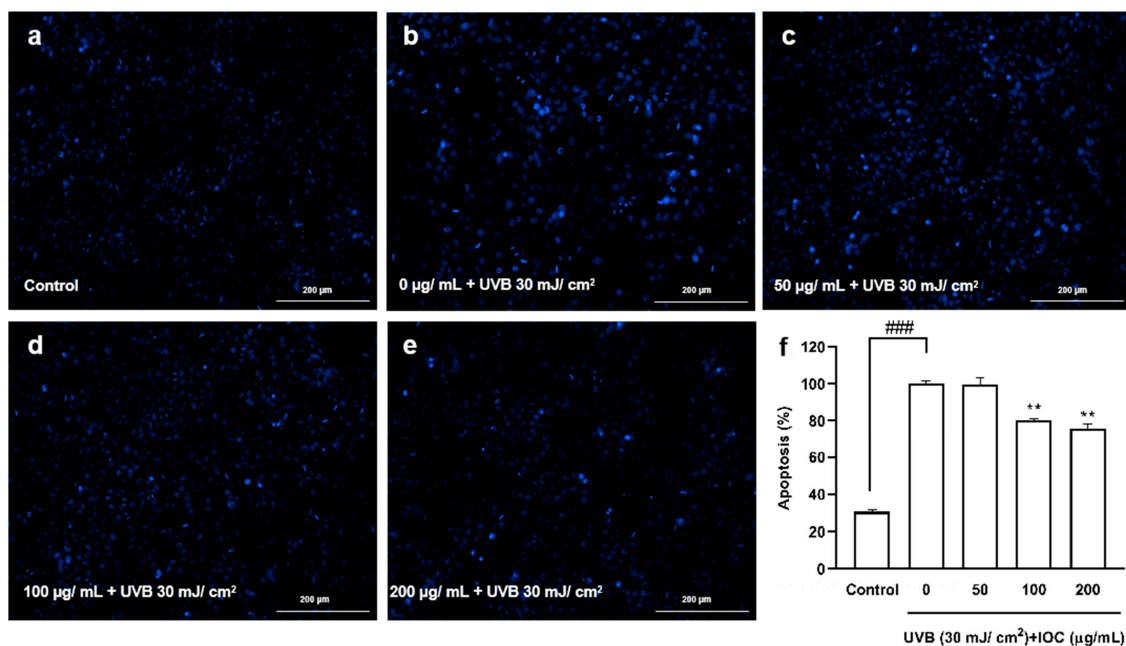


Figure 5. The protective effects of IOC against UVB-induced apoptosis in HaCaT cells. (a) Non-UVB-irradiated cells; (b) 30 mJ·cm⁻² UVB-irradiated cells; (c) cells treated with 50 $\mu\text{g}\cdot\text{mL}^{-1}$ of IOC and

UVB; (d) cells treated with $100 \mu\text{g}\cdot\text{mL}^{-1}$ of IOC and UVB; (e) cells treated with $200 \mu\text{g}\cdot\text{mL}^{-1}$ of IOC and UVB; (f) quantification of apoptotic cells. ** $p < 0.01$ as compared to the UVB-irradiated group and ### $p < 0.001$ as compared to the control group.

3.7. Effect of the IOC on UVB-Induced Antioxidant Enzyme Expression through Nrf2 Activation in HaCaT Cells

The Nrf2–Keap1 pathway plays pivotal roles in regulating the induction of antioxidant enzymes. To evaluate the effects of the IOC on UVB-irradiation-induced antioxidant enzyme expression, Western blotting was performed to analyze protein levels. Nrf2, SOD-1, and HO-1 expression was significantly inhibited following UVB irradiation. However, co-treatment with the IOC significantly restored the expression of these antioxidant enzymes in a dose-dependent manner (Figure 6a,b). Treatment with the IOC activated the Nrf2–Keap1 pathway, enhanced Nrf2 expression, and suppressed Keap1 expression. While UVB irradiation upregulated Keap1 expression, high concentrations of IOC downregulated it (Figure 6a). Therefore, the IOC inhibited intracellular ROS generation by promoting the activation of Nrf2 and inducing the expression of antioxidant enzymes, such as SOD-1 and HO-1.

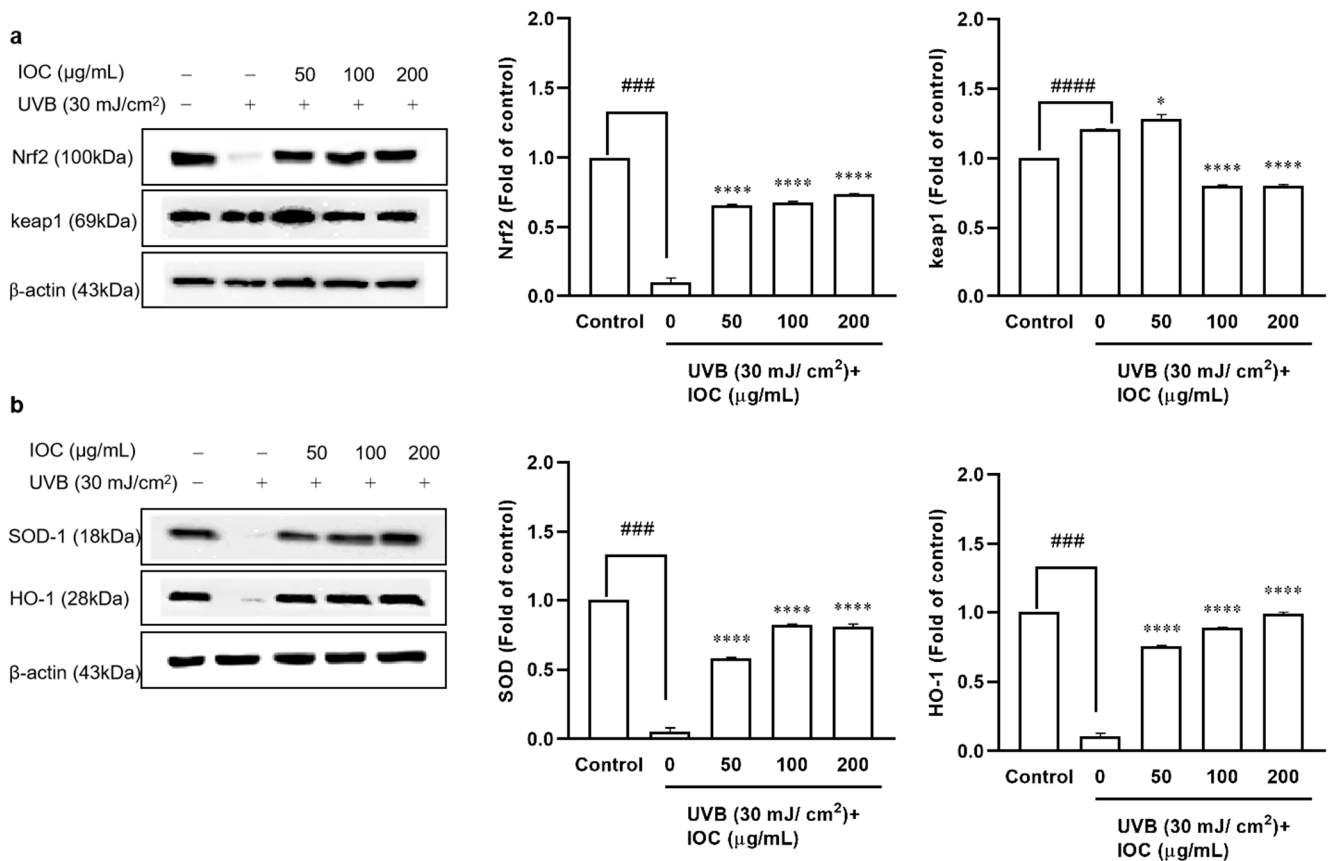


Figure 6. Effect of IOC on antioxidant-related protein in UVB-irradiated HaCaT cells. (a) Protein levels of Nrf2 and Keap1; (b) protein levels of SOD-1 and HO-1. β -actin was used as internal control. Quantification was assisted with the ImageJ software. Results are represented as mean \pm SEM. * $p < 0.05$ and **** $p < 0.0001$ as compared to the UVB-irradiated group; ### $p < 0.001$ and #### $p < 0.0001$ as compared to the control group.

3.8. Effects of IOC on MMPs Expression in UVB-Induced HaCaT Cells

Collagen acts as an important structural support system providing strength and elasticity to the skin. UVB exposure activates MMPs secretion, leading to collagen degradation, which is a hallmark of skin aging [32]. As shown in Figure 7, UVB irradiation significantly increased MMP1, 2, and 9 secretion. However, MMPs' expression decreased in a dose-dependent manner in IOC-pretreated HaCaT cells. Therefore, the IOC inhibited MMPs expression, thereby playing an anti-wrinkle role, which is important to prevent photoaging.

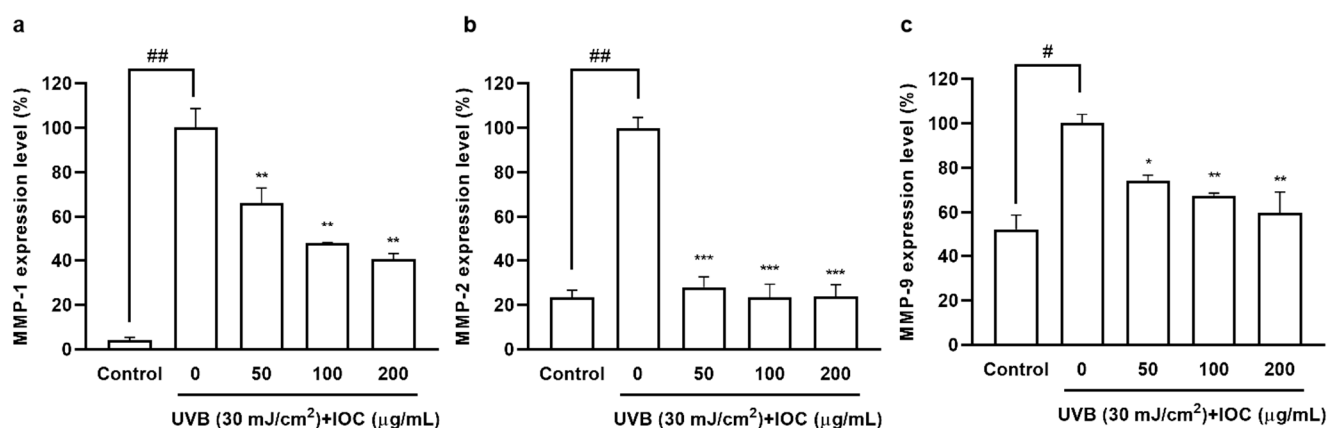


Figure 7. IOC reduces MMPs expression in UVB-irradiated HaCaT cells. (a) MMP-1 expression level in UVB-irradiated HaCaT cells; (b) MMP-2 expression level in UVB-irradiated HaCaT cells; (c) MMP-9 expression level in UVB-irradiated HaCaT cells. All experiments were triplicated, and data are expressed as the mean \pm SEM. * $p < 0.05$, ** $p < 0.01$, and *** $p < 0.001$ as compared to the UVB-irradiated group; # $p < 0.05$ and ## $p < 0.01$ as compared to the control group.

3.9. Effects of the IOC on H₂O₂-Induced Oxidative Stress in Zebrafish

A zebrafish embryonic model was used to determine the effect of the IOC on H₂O₂-induced oxidative stress in vivo. The survival rate, heart beating rate, ROS generation, and cell death of zebrafish embryos were investigated. Figure 8 illustrated that the intracellular ROS and cell death decreased in a dose-dependent manner following treatment with the IOC. Additionally, compared with the control group, it was found that the survival rate was significantly decreased when stimulated with H₂O₂. However, this survival rate increased after treatment with 100 and 200 µg·mL⁻¹ of the IOC. Furthermore, the heart beating rate of zebrafish was decreased in a dose-dependent manner in IOC-treated groups (50–200 µg·mL⁻¹) compared with that in the H₂O₂-induced group. These observations confirmed that the IOC may produce protective effects against H₂O₂-induced oxidative stress.

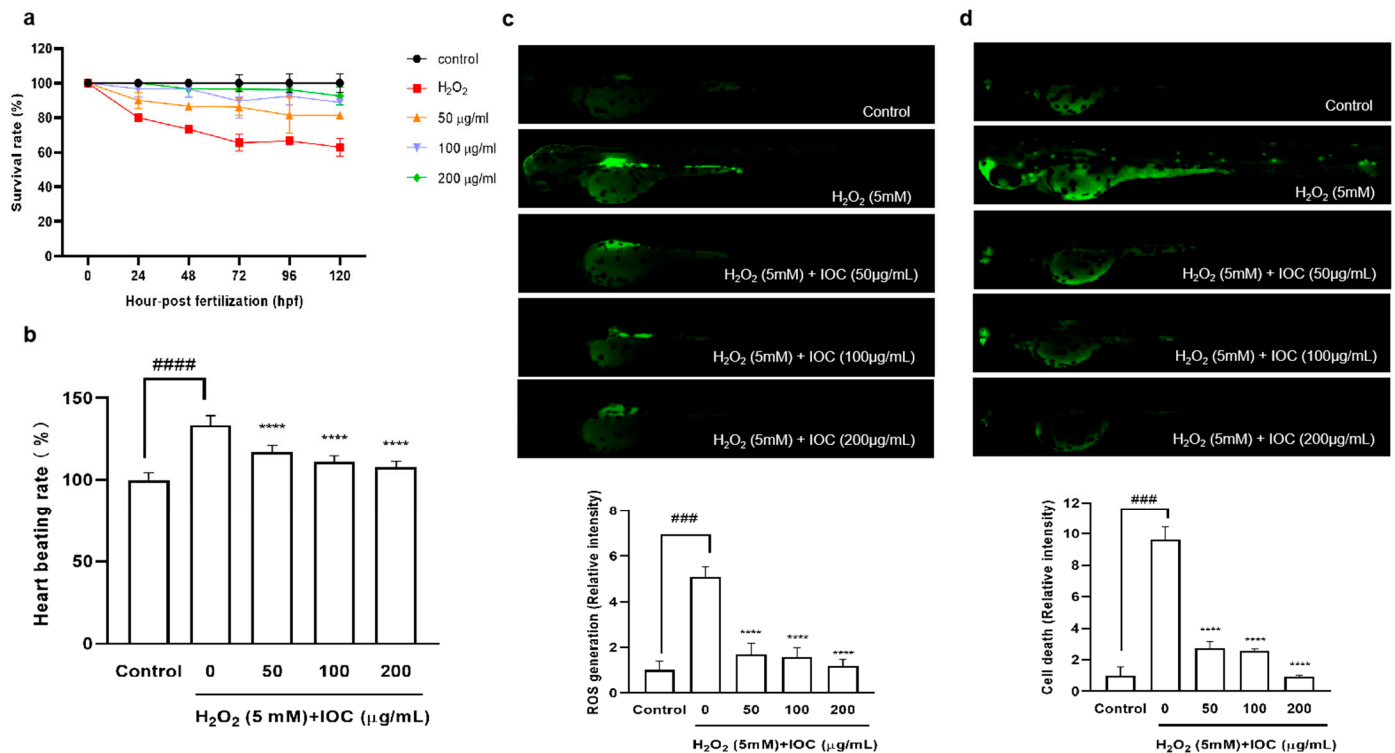


Figure 8. IOC depresses H₂O₂-induced oxidative damage in vivo in zebrafish. (a) Survival rate; (b) heart beating rate of both atrium and ventricle; (c) intracellular ROS generation; (d) cell death. All experiments were triplicated, and data are expressed as the mean ± SEM. **** $p < 0.0001$ as compared to the H₂O₂-induced group, ### $p < 0.001$ and ##### $p < 0.0001$ as compared to the control group.

4. Discussion

Among many biological processes, inflammation, oxidation, and photodamage are linked to one another. UVB radiation from the sun can activate complex biochemical reactions that induce skin damage and aging. Simultaneously, excessive UVB irradiation decreases cellular antioxidant levels, resulting in ROS accumulation [33]. When the ROS concentration exceeds the basal level, cellular defenses against oxidative stress are weakened, stimulating the expression of pro-inflammatory factors and MMPs, and leading to an inflammatory response and accelerating skin aging [34,35].

I. okamurae is an edible brown alga belonging to the *Ishige* genus of the *Ishigeaceae* family. *I. okamurae* contains a number of bioactive compounds and shows various bioactivities. For instance, Kang et al. [11] reported that isophloroglucin A derived from *I. okamurae* shows anti-obesity activity. Moreover, fucoxanthin has been reported to inhibit LPS-induced inflammatory responses in RAW 264.7 cells through the suppression of NF-κB activation and MAPK phosphorylation [14]. However, the cosmeceutical effects of the sulfated polysaccharide extract from *I. okamurae* remained to be assessed. Therefore, we used different cell lines as well as in vitro and in vivo methods to explore the cosmeceutical effects of IOC from multiple perspectives, such as anti-inflammatory, antioxidant, and photoprotective effects.

The IOC contains abundant sulfated polysaccharides (48.47%), fucose (43.50%), and glucose (36.39%). The extraction of bioactive compounds from seaweeds is restricted by the complexity of their cell wall polysaccharides. As Celluclast can degrade the seaweed cell wall, enzyme-assisted extraction helps the release of biologically active substances and contributes to increasing the content of polysaccharides and fucose in the extract [19]. As shown in Table 1, carbohydrates were concentrated during the precipitation process, and high amounts of sulfated polysaccharides were confirmed, which contributed to the cosmeceutical effects. Previous in vitro and in vivo studies have shown that sulfated polysaccharide extracts from *Hizikia fusiforme* possess antioxidant, anti-inflammatory,

and photoprotective activities [36]. Sanjeeva et al. [37] reported that fucoidan—a sulfated polysaccharide isolated from *Sargassum horneri*—produced anti-inflammatory effects in LPS-induced cells. Moreover, Kim et al. [38] demonstrated that polysaccharides isolated from *Psidium guajava* exhibited antioxidant effects; simultaneously, fucose, galactose, and rhamnose levels were increased in the sulfate polysaccharide fraction. Fucose, galactose, rhamnose, and arabinose are associated with antioxidant activity. Organic free radicals, such as DPPH, ABTS, and ORAC, are commonly used to assess antioxidant activity. Therefore, in the present study, the antioxidant activity of the IOC was evaluated using the ABTS assay. As expected, the IOC possessed potent free radical scavenging activity, particularly at the concentration of $100 \mu\text{g}\cdot\text{mL}^{-1}$. The balance between enzymatic antioxidants and free radicals is important for effective intracellular oxidative stress relief. In the present study, a significant and dose-dependent decline in intracellular ROS levels was noted following IOC treatment. Oxidative stress affects cell viability. Abundant fucose in the IOC implies greater antioxidant potential; accordingly, increasing the IOC concentration produced a protective effect against H_2O_2 -stimulated cell death in Vero cells.

Inflammation is a necessary component of physiological defense processes and is a response to cellular damage caused by oxidative stress, radiation (e.g., UV radiation), and endotoxins (e.g., LPSs) [6]. LPS, a crucial cell wall component of Gram-negative bacteria, induces an inflammatory response in macrophages, promoting the production of inflammatory mediators, such as NO, TNF- α , PGE2, IL-6, and IL-1 β [29]. Simultaneously, increased NO production promotes ROS generation, which, in turn, induces apoptosis. Oxidative stress and inflammatory responses are interrelated. Macrophage production of PGE2 and proinflammatory cytokines plays key roles in the inflammatory process. To confirm the cytotoxicity and anti-inflammatory activity of the IOC, the viability of LPS-induced RAW 264.7 macrophages and inhibition of the production of NO and PGE2, which are inflammatory response indicators, were confirmed. At all concentrations, the IOC suppressed NO secretion in LPS-stimulated RAW 264.7 cells, and PGE2 levels decreased significantly in a dose-dependent manner with increasing IOC concentrations. Similarly, Sanjeeva et al. [37] showed that fucoidan—a complex sulfated polysaccharide isolated from *Sargassum horneri*—exhibits potent anti-inflammatory activity by blocking the MAPK and NF- κB signaling pathways. In addition, Jayawardena et al. [39] demonstrated that the anti-inflammatory potential of fucoidan extracted from the brown alga *Turbinaria ornata* was assisted by enzymatic hydrolysis in both in vivo and in vitro models.

UV radiation can cause photodamage, wrinkles, and skin diseases by inducing excessive production of intracellular ROS and stimulating the expression of matrix MMPs and pro-inflammatory cytokines [34,40]. Natural aging and photoaging are the major causes of skin aging, manifesting as dryness, hyperpigmentation, laxity, and wrinkles [41]. Additionally, UV-radiation-mediated ROS production has been shown to promote the expression of specific genes involved in signaling pathways, resulting in various physiological effects, such as inflammatory responses. Increased ROS and H_2O_2 concentrations activate the NF- κB pathway, thereby increasing PGE2 and cytokine levels [6,35]. Therefore, we examined the inhibitory effects of the IOC on wrinkling-related enzymes. The increased activity of skin enzymes, such as collagenase, elastase, and HAase, leads to the proteolysis of the extracellular matrix (ECM). Furthermore, upregulated expression of MMPs, particularly MMP-2 and MMP-9, can lead to ECM degradation. Another important collagenase is MMP-1, which mainly degrades type I and type III collagen [36]. Chronic UV exposure denatures collagen and enzymes in the dermis, and elastin and collagen degradation results in the loss of skin elasticity and reduction in skin thickness, respectively. These are the major reasons for skin aging and wrinkling [24,42,43]. Our results showed that the IOC produced inhibitory effects on collagenase, elastase, and HAase and dose-dependently downregulated the expression of MMP-1, MMP-2, and MMP-9. Therefore, the IOC may act as a potential anti-wrinkle agent by interrupting the degradation of these skin enzymes under UV exposure. HaCaT cells, which are immortalized human keratinocytes, are widely used to study epidermal homeostasis. Therefore, we investigated the photoprotective

activity of the IOC following UVB stimulation of HaCaT cells. The protective effects of the IOC against UVB irradiation were observed through cell viability assays. Our experiments revealed strong photoprotective activity of the IOC. As such, IOC treatment delayed skin aging by downregulating ROS production and protecting against nuclear fragmentation in UVB-stimulated HaCaT cells.

Nearly 80% of ROS production is induced by UV radiation. Therefore, antioxidant substances are critical for inhibiting oxidative damage and protecting the skin from photodamage. Activation of the Nrf2–Keap1 signaling pathway maintains high levels of antioxidant enzymes, such as SOD-1 and HO-1, which play pivotal roles in protection against photoaging [44]. The IOC significantly enhanced the levels of SOD-1 and HO-1 antioxidants through upregulating Nrf2 expression and significantly downregulating Keap1 expression. Therefore, the IOC produced protective effects against UVB-induced oxidative damage and apoptosis in HaCaT cells, primarily through the activation of the Nrf2 signaling pathway. In a similar study, Oh et al. [45] showed that 3,5-dicaffeoyl-epiquinic acid reduced oxidative stress and prevented photoaging through upregulation of the antioxidant enzyme transcription factor Nrf2. These results imply that the IOC can serve as an effective skin protective ingredient in cosmetics.

ROS plays a significant role in oxidative stress, causing the breakdown of DNA, proteins, cell membranes, and other constituents. The accumulation of molecular damage leads to apoptosis, necrosis, and death. H₂O₂ is associated with the formation of hydroxyl and singlet oxygen radicals, which can stimulate intracellular ROS production and cause cell damage and senescence [46,47]. As a result, antioxidative substances are critical for preventing oxidative stress. Antioxidants in cosmeceuticals play critical roles in suppressing and inhibiting oxidative damage reactions. Therefore, the *in vivo* antioxidant effects of the IOC were investigated in a zebrafish embryo model. Because of their suitability for studying human disease processes and development, zebrafish are considered a painless *in vitro* alternative, becoming one of the most widely used vertebrate models [48]. Following H₂O₂ stimulation, excess intracellular ROS are generated, leading to cell death. A dose-dependent reduction in ROS levels and remarkably reduced cell death rate were observed in zebrafish following treatment with the IOC. The survival rate of H₂O₂-stimulated zebrafish was significantly decreased; however, the rate increased following co-treatment with IOC. In addition, H₂O₂ stimulation caused heartbeat disorder in zebrafish; however, co-treatment with IOC effectively downregulated the heart rate of zebrafish. In summary, our *in vitro* and *in vivo* results indicate that the IOC possesses potent anti-inflammatory and antioxidant activities and presents photoprotective potential.

5. Conclusions

We investigated the effect of sulfated polysaccharides from Celluclast-assisted extract of the brown seaweed *I. okamurae* as a source of natural cosmetic ingredients. IOC produced protective effects against H₂O₂-induced oxidative stress both *in vitro* (Vero cells) and *in vivo* (zebrafish). Furthermore, IOC produced anti-inflammatory effects in RAW 264.7 macrophages, and IOC exhibited antioxidant, anti-wrinkle, and photoprotective effects by suppressing UVB-induced oxidative stress, activating the Nrf2–Keap1 signaling pathway, and reducing MMPs expression in HaCaT cells. Therefore, the IOC may be used as an effective ingredient in the functional food and cosmetic industries.

Author Contributions: Conceptualization, F.Y. and Y.-J.J.; methodology, F.Y., J.H., D.P.N. and Y.M.K.; software, F.Y. and D.P.N.; validation, F.Y. and J.H.; investigation, F.Y., M.-S.H. and Y.M.K.; resources, Y.-J.J.; data curation, F.Y. and J.H.; supervision, Y.-J.J. and M.-S.H.; writing—original draft preparation, F.Y.; writing—review and editing, F.Y. and Y.-J.J.; funding acquisition, Y.-J.J. All authors have read and agreed to the published version of the manuscript.

Funding: This work was supported by the 2022 education, research, and student guidance grant funded by Jeju National University.

Institutional Review Board Statement: The zebrafish experiment was approved by the Animal Care and Use Committee of Jeju National University (Approval No. 2020-0049).

Informed Consent Statement: Not applicable.

Data Availability Statement: The data are contained within the article.

Conflicts of Interest: The authors declare no conflict of interest.

References

1. Sahoo, B.M.; Banik, B.K.; Borah, P.; Jain, A. Reactive oxygen species (ROS): Key components in cancer therapies. *Anti-Cancer Agents Med. Chem.* **2022**, *22*, 215–222. [[CrossRef](#)]
2. Aslam, A.; Bahadar, A.; Liaquat, R.; Saleem, M.; Waqas, A.; Zwawi, M. Algae as an attractive source for cosmetics to counter environmental stress. *Sci. Total Env.* **2021**, *772*, 144905. [[CrossRef](#)]
3. Juan, C.A.; Pérez de la Lastra, J.M.; Plou, F.J.; Pérez-Lebeña, E. The Chemistry of Reactive Oxygen Species (ROS) Revisited: Outlining Their Role in Biological Macromolecules (DNA, Lipids and Proteins) and Induced Pathologies. *Int. J. Mol. Sci.* **2021**, *22*, 4642. [[CrossRef](#)] [[PubMed](#)]
4. Liu, T.; Sun, L.; Zhang, Y.; Wang, Y.; Zheng, J. Imbalanced GSH/ROS and sequential cell death. *J. Biochem. Mol. Toxicol.* **2022**, *36*, e22942. [[CrossRef](#)]
5. Liu, Z.; Ren, Z.; Zhang, J.; Chuang, C.-C.; Kandaswamy, E.; Zhou, T.; Zuo, L. Role of ROS and nutritional antioxidants in human diseases. *Front. Physiol.* **2018**, *9*, 477. [[CrossRef](#)] [[PubMed](#)]
6. Kageyama, H.; Waditee-Sirisattha, R. Antioxidative, Anti-Inflammatory, and Anti-Aging Properties of Mycosporine-Like Amino Acids: Molecular and Cellular Mechanisms in the Protection of Skin-Aging. *Mar. Drugs* **2019**, *17*, 222. [[CrossRef](#)]
7. Wang, L.; Kim, H.S.; Oh, J.Y.; Je, J.G.; Jeon, Y.-J.; Ryu, B. Protective effect of diphlorethohydroxycarmalol isolated from *Ishige okamurae* against UVB-induced damage in vitro in human dermal fibroblasts and in vivo in zebrafish. *Food Chem. Toxicol.* **2020**, *136*, 110963. [[CrossRef](#)] [[PubMed](#)]
8. Nduka, J.K.; Kelle, H.I.; Odiba, I.O. Review of health hazards and toxicological effects of constituents of cosmetics. In *Poisoning in the Modern World-New Tricks for an Old Dog?* IntechOpen: London, UK, 2019; pp. 59–76.
9. Lomartire, S.; Gonçalves, A.M.M. An Overview of Potential Seaweed-Derived Bioactive Compounds for Pharmaceutical Applications. *Mar. Drugs* **2022**, *20*, 141. [[CrossRef](#)]
10. Pradhan, B.; Bhuyan, P.P.; Patra, S.; Nayak, R.; Behera, P.K.; Behera, C.; Behera, A.K.; Ki, J.-S.; Jena, M. Beneficial effects of seaweeds and seaweed-derived bioactive compounds: Current evidence and future prospective. *Biocatal. Agric. Biotechnol.* **2022**, *39*, 102242. [[CrossRef](#)]
11. Kang, N.; Oh, S.; Kim, H.-S.; Ahn, H.; Choi, J.; Heo, S.-J.; Byun, K.; Jeon, Y.-J. Ishophloroglucin A, derived from *Ishige okamurae*, regulates high-fat-diet-induced fat accumulation via the leptin signaling pathway, associated with peripheral metabolism. *Algal. Res.* **2020**, *50*, 101974. [[CrossRef](#)]
12. Jimenez-Lopez, C.; Pereira, A.G.; Lourenço-Lopes, C.; Garcia-Oliveira, P.; Cassani, L.; Fraga-Corral, M.; Prieto, M.A.; Simal-Gandara, J. Main bioactive phenolic compounds in marine algae and their mechanisms of action supporting potential health benefits. *Food Chem.* **2021**, *341*, 128262. [[CrossRef](#)] [[PubMed](#)]
13. Julião, D.R.; Afonso, C.; Gomes-Bispo, A.; Bandarra, N.M.; Cardoso, C. The effect of drying on undervalued brown and red seaweed species: Bioactivity alterations. *Phycol. Res.* **2021**, *69*, 246–257. [[CrossRef](#)]
14. Kim, K.-N.; Heo, S.-J.; Yoon, W.-J.; Kang, S.-M.; Ahn, G.; Yi, T.-H.; Jeon, Y.-J. Fucoxanthin inhibits the inflammatory response by suppressing the activation of NF- κ B and MAPKs in lipopolysaccharide-induced RAW 264.7 macrophages. *Eur. J. Pharm.* **2010**, *649*, 369–375. [[CrossRef](#)] [[PubMed](#)]
15. Wang, L.; Kim, H.S.; Je, J.-G.; Oh, J.Y.; Kim, Y.-S.; Cha, S.-H.; Jeon, Y.-J. Protective Effect of Diphlorethohydroxycarmalol Isolated from *Ishige okamurae* Against Particulate Matter-Induced Skin Damage by Regulation of NF- κ B, AP-1, and MAPKs Signaling Pathways In Vitro in Human Dermal Fibroblasts. *Molecules* **2020**, *25*, 1055. [[CrossRef](#)]
16. Kim, M.-S.; Oh, G.-W.; Jang, Y.-M.; Ko, S.-C.; Park, W.-S.; Choi, I.-W.; Kim, Y.-M.; Jung, W.-K. Antimicrobial hydrogels based on PVA and diphlorethohydroxycarmalol (DPHC) derived from brown alga *Ishige okamurae*: An in vitro and in vivo study for wound dressing application. *Mater. Sci. Eng.* **2020**, *107*, 110352. [[CrossRef](#)]
17. Kim, S.-Y.; Ahn, G.; Kim, H.-S.; Je, J.-G.; Kim, K.-N.; Jeon, Y.-J. Diphlorethohydroxycarmalol (DPHC) Isolated from the Brown Alga *Ishige okamurae* Acts on Inflammatory Myopathy as an Inhibitory Agent of TNF- α . *Mar. Drugs* **2020**, *18*, 529. [[CrossRef](#)]
18. Li, B.B.; Smith, B.; Hossain, M.M. Extraction of phenolics from citrus peels: II. Enzyme-assisted extraction method. *Sep. Purif. Technol.* **2006**, *48*, 189–196. [[CrossRef](#)]
19. Quitério, E.; Grosso, C.; Ferraz, R.; Delerue-Matos, C.; Soares, C. A Critical Comparison of the Advanced Extraction Techniques Applied to Obtain Health-Promoting Compounds from Seaweeds. *Mar. Drugs* **2022**, *20*, 677. [[CrossRef](#)]
20. Saito, H.; Yamagata, T.; Suzuki, S. Enzymatic Methods for the Determination of Small Quantities of Isomeric Chondroitin Sulfates. *J. Biol. Chem.* **1968**, *243*, 1536–1542. [[CrossRef](#)]
21. Chandler, S.F.; Dodds, J.H. The effect of phosphate, nitrogen and sucrose on the production of phenolics and solasodine in callus cultures of *solanum laciniatum*. *Plant Cell Rep.* **1983**, *2*, 205–208. [[CrossRef](#)]

22. DuBois, M.; Gilles, K.A.; Hamilton, J.K.; Rebers, P.A.; Smith, F. Colorimetric Method for Determination of Sugars and Related Substances. *Anal. Chem.* **1956**, *28*, 350–356. [[CrossRef](#)]
23. Re, R.; Pellegrini, N.; Proteggente, A.; Pannala, A.; Yang, M.; Rice-Evans, C. Antioxidant activity applying an improved ABTS radical cation decolorization assay. *Free Radic. Biol. Med.* **1999**, *26*, 1231–1237. [[CrossRef](#)] [[PubMed](#)]
24. Wang, L.; Oh, J.Y.; Yang, H.-W.; Kim, H.S.; Jeon, Y.-J. Protective effect of sulfated polysaccharides from a Celluclast-assisted extract of *Hizikia fusiforme* against ultraviolet B-induced photoaging in vitro in human keratinocytes and in vivo in zebrafish. *Mar. Life Sci. Technol.* **2019**, *1*, 104–111. [[CrossRef](#)]
25. Kraunsoe, J.A.E.; Claridge, T.D.W.; Lowe, G. Inhibition of Human Leukocyte and Porcine Pancreatic Elastase by Homologues of Bovine Pancreatic Trypsin Inhibitor. *Biochemistry* **1996**, *35*, 9090–9096. [[CrossRef](#)] [[PubMed](#)]
26. Elson, L.A.; Morgan, W.T.J. A colorimetric method for the determination of glucosamine and chondrosamine. *Biochem. J.* **1933**, *27*, 1824. [[CrossRef](#)] [[PubMed](#)]
27. Yang, X.; Kang, M.-C.; Lee, K.-W.; Kang, S.-M.; Lee, W.-W.; Jeon, Y.-J. Antioxidant activity and cell protective effect of loliolide isolated from *Sargassum ringgoldianum* subsp. *coreanum*. *Algae* **2011**, *26*, 201–208. [[CrossRef](#)]
28. Kim, H.-S.; Shin, B.-O.; Kim, S.-Y.; Wang, L.; Lee, W.; Kim, Y.T.; Rho, S.; Cho, M.; Jeon, Y.-J. Antioxidant activity of pepsin hydrolysate derived from edible *Hippocampus abdominalis* in vitro and in zebrafish models. *Korean J. Fish. Aquat. Sci.* **2016**, *49*, 445–453. [[CrossRef](#)]
29. Wang, L.; Oh, J.Y.; Fernando, S.; Sanjeeva, K.A.; Kim, E.-A.; Lee, W.; Jeon, Y.-J. Soft corals collected from Jeju Island; a potential source of anti-inflammatory phytochemicals. *J. Chitin Chitosan* **2016**, *21*, 247–254. [[CrossRef](#)]
30. Ko, J.-Y.; Kim, E.-A.; Lee, J.-H.; Kang, M.-C.; Lee, J.-S.; Kim, J.-S.; Jung, W.-K.; Jeon, Y.-J. Protective effect of aquacultured flounder fish-derived peptide against oxidative stress in zebrafish. *Fish Shellfish. Immunol.* **2014**, *36*, 320–323. [[CrossRef](#)]
31. Fernando, I.P.S.; Sanjeeva, K.K.A.; Kim, H.-S.; Kim, S.-Y.; Lee, S.-H.; Lee, W.W.; Jeon, Y.-J. Identification of sterols from the soft coral *Dendronephthya gigantea* and their anti-inflammatory potential. *Environ. Toxicol. Pharm.* **2017**, *55*, 37–43. [[CrossRef](#)]
32. Fisher, G.J.; Kang, S.; Varani, J.; Bata-Csorgo, Z.; Wan, Y.; Datta, S.; Voorhees, J.J. Mechanisms of Photoaging and Chronological Skin Aging. *Arch. Dermatol.* **2002**, *138*, 1462–1470. [[CrossRef](#)] [[PubMed](#)]
33. Pourzand, C.; Albiéri-Borges, A.; Raczek, N.N. Shedding a New Light on Skin Aging, Iron- and Redox-Homeostasis and Emerging Natural Antioxidants. *Antioxidants* **2022**, *11*, 471. [[CrossRef](#)] [[PubMed](#)]
34. Zhang, D.; Lu, C.; Yu, Z.; Wang, X.; Yan, L.; Zhang, J.; Li, H.; Wang, J.; Wen, A. Echinacoside alleviates UVB irradiation-mediated skin damage via inhibition of oxidative stress, DNA damage, and apoptosis. *Oxid Med. Cell. Longev.* **2017**, *2017*, 6851464. [[CrossRef](#)] [[PubMed](#)]
35. Jordan, C.T.; Hilt, J.Z.; Dziubla, T.D. Polyphenol conjugated poly (beta-amino ester) polymers with hydrogen peroxide triggered degradation and active antioxidant release. *J. Appl. Polym. Sci.* **2020**, *137*, 48647. [[CrossRef](#)]
36. Wang, L.; Lee, W.; Oh, J.Y.; Cui, Y.R.; Ryu, B.; Jeon, Y.-J. Protective Effect of Sulfated Polysaccharides from Celluclast-Assisted Extract of *Hizikia fusiforme* Against Ultraviolet B-Induced Skin Damage by Regulating NF- κ B, AP-1, and MAPKs Signaling Pathways In Vitro in Human Dermal Fibroblasts. *Mar. Drugs* **2018**, *16*, 239. [[CrossRef](#)]
37. Sanjeeva, K.K.A.; Jayawardena, T.U.; Kim, S.-Y.; Kim, H.-S.; Ahn, G.; Kim, J.; Jeon, Y.-J. Fucoidan isolated from invasive *Sargassum horneri* inhibit LPS-induced inflammation via blocking NF- κ B and MAPK pathways. *Algal. Res.* **2019**, *41*, 101561. [[CrossRef](#)]
38. Kim, S.-Y.; Kim, E.-A.; Kim, Y.-S.; Yu, S.-K.; Choi, C.; Lee, J.-S.; Kim, Y.-T.; Nah, J.-W.; Jeon, Y.-J. Protective effects of polysaccharides from *Psidium guajava* leaves against oxidative stresses. *Int. J. Biol. Macromol.* **2016**, *91*, 804–811. [[CrossRef](#)]
39. Jayawardena, T.U.; Fernando, I.P.S.; Lee, W.W.; Sanjeeva, K.K.A.; Kim, H.-S.; Lee, D.-S.; Jeon, Y.-J. Isolation and purification of fucoidan fraction in *Turbinaria ornata* from the Maldives; Inflammation inhibitory potential under LPS stimulated conditions in in-vitro and in-vivo models. *Int. J. Biol. Macromol.* **2019**, *131*, 614–623. [[CrossRef](#)]
40. Ries, C.; Egea, V.; Karow, M.; Kolb, H.; Jochum, M.; Neth, P. MMP-2, MT1-MMP, and TIMP-2 are essential for the invasive capacity of human mesenchymal stem cells: Differential regulation by inflammatory cytokines. *Blood* **2007**, *109*, 4055–4063. [[CrossRef](#)]
41. Gu, Y.; Han, J.; Jiang, C.; Zhang, Y. Biomarkers, oxidative stress and autophagy in skin aging. *Ageing Res. Rev.* **2020**, *59*, 101036. [[CrossRef](#)]
42. Maity, N.; Nema, N.K.; Abedy, M.K.; Sarkar, B.K.; Mukherjee, P.K. Exploring *Tagetes erecta* Linn flower for the elastase, hyaluronidase and MMP-1 inhibitory activity. *J. Ethnopharmacol.* **2011**, *137*, 1300–1305. [[CrossRef](#)] [[PubMed](#)]
43. Azmi, N.; Hashim, P.; Hashim, D.M.; Halimoon, N.; Majid, N.M.N. Anti-elastase, anti-tyrosinase and matrix metalloproteinase-1 inhibitory activity of earthworm extracts as potential new anti-aging agent. *Asian Pac. J. Trop. Biomed.* **2014**, *4*, S348–S352. [[CrossRef](#)] [[PubMed](#)]
44. Park, C.; Park, J.; Kim, W.-J.; Kim, W.; Cheong, H.; Kim, S.-J. Malonic Acid Isolated from *Pinus densiflora* Inhibits UVB-Induced Oxidative Stress and Inflammation in HaCaT Keratinocytes. *Polymers* **2021**, *13*, 816. [[CrossRef](#)] [[PubMed](#)]
45. Oh, J.H.; Karadeniz, F.; Lee, J.I.; Seo, Y.; Kong, C.S. Protective effect of 3,5-dicaffeoyl-epi-quinic acid against UVB-induced photoaging in human HaCaT keratinocytes. *Mol. Med. Rep.* **2019**, *20*, 763–770. [[CrossRef](#)]
46. Karapetsas, A.; Voulgaridou, G.-P.; Konialis, M.; Tsochantaridis, I.; Kynigopoulos, S.; Lambropoulou, M.; Stavropoulou, M.-I.; Stathopoulou, K.; Aligiannis, N.; Bozidis, P.; et al. Propolis Extracts Inhibit UV-Induced Photodamage in Human Experimental In Vitro Skin Models. *Antioxidants* **2019**, *8*, 125. [[CrossRef](#)]

47. Jiratchayamaethasakul, C.; Ding, Y.; Hwang, O.; Im, S.-T.; Jang, Y.; Myung, S.-W.; Lee, J.M.; Kim, H.-S.; Ko, S.-C.; Lee, S.-H. In vitro screening of elastase, collagenase, hyaluronidase, and tyrosinase inhibitory and antioxidant activities of 22 halophyte plant extracts for novel cosmeceuticals. *Fish. Aquat. Sci.* **2020**, *23*, 6. [[CrossRef](#)]
48. Watzke, J.; Schirmer, K.; Scholz, S. Bacterial lipopolysaccharides induce genes involved in the innate immune response in embryos of the zebrafish (*Danio rerio*). *Fish Shellfish Immunol.* **2007**, *23*, 901–905. [[CrossRef](#)]